



HHS Public Access

Author manuscript

Transl Res Anat. Author manuscript; available in PMC 2022 September 20.

Published in final edited form as:

Transl Res Anat. 2022 June ; 27: . doi:10.1016/j.tria.2022.100171.

Extended reality visualization of medical museum specimens: Online presentation of conjoined twins curated by Dr. Jacob Henle between 1844–1852

Brandi S. Mikami^{a,*}, Thomas E. Hynd^b, U-Young Lee^{a,c}, J. DeMeo^a, Jesse D. Thompson^a, Roman Sokiranski^d, Sara Doll^e, Scott Lozanoff^a

^aDepartment of Anatomy, Biochemistry & Physiology, John A. Burns School of Medicine, Honolulu, HI, 96813, USA

^bDepartment of Biology, James Madison University, Harrisonburg, VA, 22807, USA

^cDepartment of Anatomy, Catholic University of Korea, Seoul, KR, 06591, South Korea

^dDepartment of Anatomy & Cell Biology, Medical University of Varna, Varna, BG-9002, Bulgaria

^eDepartment of Anatomy and Cell Biology, University of Heidelberg, Heidelberg, DE, 69120, USA

Abstract

Background: The purpose of this study is to characterize a full-term conjoined twins' cadaver curated by Dr. Jacob Henle sometime between 1844 and 1852 and demonstrate digital distribution of an old and rare medical museum specimen using an extended reality (XR) model workflow.

Methods: The cadaver (Preparation 296) is in the Department of Anatomy and Cell Biology at the University of Heidelberg. An XR display workflow comprises image capture, segmentation, and visualization using CT/MR scans derived from the cadaver. Online radiology presentation to medical students focuses on diagnostic characteristics of anatomical systems depicted with XR models.

Results: Developmental defects in Preparation 296 include duplicated supradiaphragmatic structures and abnormal osteological features. Subdiaphragmatically, the gut is continuous on the right, but terminates at the distal esophagus on the left. One large liver occupies the abdomen with

This is an open access article under the CC BY-NC-ND license (<http://creativecommons.org/licenses/by-nc-nd/4.0/>).

*Corresponding author. Department of Anatomy, Biochemistry & Physiology, John A. Burns School of Medicine, 651 Ilalo Street, Honolulu, HI, 96813, USA. mikamib@hawaii.edu (B.S. Mikami).

CRedit authorship contribution statement

Brandi S. Mikami: Conceptualization, Formal analysis, Writing, Methodology. **Thomas E. Hynd:** Writing, Supervision. **U-Young Lee:** Visualization, Formal analysis. **J. DeMeo:** Formal analysis. **Jesse D. Thompson:** Data curation, Methodology. **Roman Sokiranski:** Visualization, Validation. **Sara Doll:** Resources, Data curation. **Scott Lozanoff:** Conceptualization, Writing, Supervision.

Editor conflict of interest statement

Given Dr. Scott Lozanoff's role as Editorial Board Member/Associate Editor/Editor-in-chief, had no involvement in the peer-review of this article and has no access to information regarding its peer-review.

Declaration of competing interest

There are no other financial interests or COI among all other authors.

Ethical statement

IRB exemption was applied (University of Heidelberg) based on the rationale that the identity of the twins could not be ascertained since personal identifiable information does not exist.

one spleen located on the left side. Observations suggest duplication of the primitive streak and separate notochords rostrally. Duplication occurs near the yolk sac and involves midgut formation while secondary midline fusion of the upper extremities and ribs likely results from the proximity of the embryos during development. Medical students access the model with device agnostic software during the curricular topic “Human Body Plan” that includes embryology concepts covering mechanisms of twinning.

Conclusions: The workflow enables ease-of-access XR visualizations of an old and rare museum specimen. This study also demonstrates digital distribution and utilization of XR models applicable to embryology education.

Keywords

Conjoined twins; XR anatomy; Medical museum specimens; Jacob Henle

1. Introduction

Cadaveric specimens of conjoined twins are important in anatomical collections since they provide historical, medical, social, and esthetic value to a medical museum [1,2]. Utilization of these museum specimens arise, in part, from the usefulness for understanding the adult body plan and deficiencies that result from morphogenetic dysregulation and birth defects [3]. Limited access to museum specimens can result due to fragility, as well as geographical restrictions. Efforts to increase access to museum specimens through online distribution are reported [4–6]. Various workflows for creating online models of museum specimens are particularly useful for 3D imaging [7–11]. However, hardware or software requirements impose limitations. Application of electronic visualization for depicting developmental abnormalities in anatomical specimens housed in medical museums and delivered through hardware independent methods has received little attention.

Extended reality (XR) visualization is a generalized term applied to immersive technology that merges physical and virtual experiences. The global augmented and virtual reality healthcare market size is expected to reach \$9.5 billion (USD) by 2028 [12]. XR is particularly attractive for understanding anatomy and embryology since the user can manipulate complex three-dimensional relationships [13]. Problem based learning pedagogy utilizes and delivers XR models online [14–16]. Revealing concealed anatomical information contained in old and rare museum specimens with online educational delivery platforms utilizing XR technology should evoke student interest and engagement.

The University of Heidelberg represents one such setting and houses an extensive collection of extremely unique fetal cadavers with rare developmental abnormalities. One cadaver in particular, Preparation 296, is of considerable interest. Dr. Friedrich Gustav Jacob Henle (1809–1885), a former Professor of Anatomy at the University of Heidelberg and whose name is applied to the renal tubules that he discovered, i.e., Henle’s loop, or ansa nephroni [17], curated the cadaver sometime between 1844 and 1852. Thus, this parapagus dicephalus tribrachus dipus cadaver has existed in the collection for over 150 years. Old and rare museum specimens link past and present and support learning topics surrounding historical figures in medicine. Specimens facilitate critical examination of anatomical normalization

that serves as a rationale to surgically separate conjoined twins regardless of family or patient preferences [18]. These topics extend beyond the obvious tuition concerning anatomy and embryology.

The overall purpose of this study is to implement a workflow for digital distribution of XR models derived from museum specimens using device agnostic software. To achieve this objective, a rare, conjoined twins' cadaver (Preparation 296, Anatomy Museum, University of Heidelberg) is subjected to biomedical imaging and a detailed anatomical analysis of developing systems is performed. A novel workflow facilitates creation of ease-of-use XR models digitally distributed as a case report. Parameters necessary for online delivery, as well as a trial of visualization platforms as a means of communicating case-based embryology instruction is determined.

2. Materials and methods

This study utilizes a single parapagus dicephalus tribrachus dipus conjoined twins' cadaver from the Anatomy Museum, University of Heidelberg. The fixative likely consisted of a high alcohol concentration liquid called "Weingeist," which was commonly used to store specimens in the 19th century, then transferred to formaldehyde in the 20th century. There is no indication of perfusion fixation. Dr. Henle curated the specimen while he was a professor at the University of Heidelberg sometime between 1844 and 1852 (Fig. 1A) and documentation is present in the historical archives (Fig. 1B). Personal identifiable information does not exist, and this study is IRB exempt (University of Heidelberg). The analysis applies a novel graphics workflow (Fig. 2) consisting of 1) Image Capture; 2) Segmentation and Modeling; and 3) XR Visualization followed anatomical analysis of the developing systems. A case presentation included this information and was distributed digitally in the "Human Body Plan" that is a 2-h online presentation in the anatomy block for first year medical students.

2.1. Graphics workflow

Image Capture: The cadaver, enclosed in a glass container, was photographed from all sides and labeled. The cadaver was prepared for scanning by removal from the formalin-filled container, cleaned under running tap water, and carefully inverted to remove any additional liquid. Following the measurement of vertex-breech and crown-heel lengths, the cadaver was placed in the supine position in a Styrofoam holder. MR scanning utilized a head coil with high-resolution sequences with a 1.5 T scanner and Siemens MAGNETOM Aera.¹ A Siemens dual-source CT scanner SOMATOM Force² enabled the CT examination. The cadaver was immediately placed into the container to prevent desiccation during transport and was subsequently placed back in storage. Uploading of files comprising the CT and MR datasets used a secondary mass storage device.

¹Variable slice thickness from 0.5 to 1.5 mm.

²Tube 2 × Vectron™ X-ray tube; 2 × Stellar Infinity detector with 3D anti-scatter collimator; Number of shifts acquired 384 (2 × 192); Rotation time up to 0.25 s; Temporal resolution up to 66 ms; Generator power 240 kW (2 × 120 kW); kV values 70–150 kV, adjustable in steps of 10 kV; Spatial resolution 0.24 mm; Max. Scan speed 737 mm/s with Turbo Flash.

Segmentation and Modeling: Thresholding and selected tools (region growing, smart split, and Boolean operators) from the Mimics toolbox (version 21.0, Materialise, Belgium) facilitated extraction of relevant tissue borders. Whole-body CT images provided skin surface and osteological feature extraction. Assessment of vertebral variations and the fusion of the upper limb bones also used CT scans while the T1 MRI images enabled sufficient resolution to segment internal organs. Negative airspace opacification in the CT scans enabled extraction of tissue borders for the nasal cavity, oral cavity, pharynx, larynx, trachea, esophagus, part of the digestive tract, umbilical cord, vagina, and rectum. The MR scans provided visualization of internal organ boundaries for segmentation of hearts, lungs, thymuses, aorta, liver, portal veins, hepatic veins, spleen, kidneys, vagina and urinary bladder.

Polymesh segments were exported as .STL format from each modality (MRI, CT) and imported into Pixologic Zbrush while the ribcage and skulls served as landmarks for alignment and scaling. Sculpting brushes corrected other misalignments between each series of poly meshes. Models were retopologized projecting the surface information from the original data to subdivided models, and a surface polishing algorithm was applied to retain landmarks but remove noise and faceting from corresponding segmentations. Manual editing, where necessary, removed areas with excessive noise or distortion.

Textures received additional processing to achieve high surface fidelity. Decimation was performed in Zbrush to reduce vertex counts to below 75,000 per structure, but occasionally as low as 5000 enabling accelerated rendering. Re-topology in quad geometry and UV unwrapping facilitated increased levels of surface detail for procedurally generated models. Normal, Albedo, Ambient Occlusion, Metallic, and Gloss textures maps achieved high-density surfaces for use with lower density UV unwrapped models. Texture “baking” with Adobe Substance Painter provided a final surface wrap. Models and texture exports were uploaded to Sketchfab (www.sketchfab.com) where additional material properties, lighting, and annotations were defined and applied. Transfer of models to Unity facilitated visualization with XR hardware systems including Hololens, zSpace and WebGL apps.

2.2. Anatomical analysis

The image files and models of each anatomical system (General Findings, Osteology, Cardiopulmonary, Digestive, Urogenital) were visualized and assessed for presence/absence of developing features. If present, the quantity and quality of development was characterized. Age estimation utilizing the dentition followed Schour & Massler [19], Eli et al. [20], Proffit et al. [21], and AlQahtani et al., [22].

2.3. Presentation

MR and CT uploads placed the datasets in the University of Heidelberg organizational workspace within the Rad3D platform. Students access the datasets using a beta web browser to load the real time volume models as WebGL2 and WebVR libraries. Thus, online collaborative web accessibility achieves interactive volumetric scan visualization on zSpace computers. Models are simultaneously viewable on a Hololens head-tracking 3D XR display. Complex spatial relationships were viewable in multidimensional space. The

radiology report viewed by the students used case information and categorized as Subject, History, Causes, and Complications. Embedded links directed students to the XR models of the conjoined twins visualized with Sketchfab or zSpace computers as well as other external links related to conjoined twinning.

An introductory online module presented the models as a case report within the context of the “Human Body Plan” topic. The live streaming system used Open Broadcasting Software (OBS) in conjunction with HDMI capture cards. Audio was captured via a Yamaha audio mixing board and Rode wireless microphones. The primary video input employed a Sony A7 series mirrorless camera system with aftermarket variable zoom lenses and accessories including a teleprompter. Chroma-key paint covered a wall in the dissecting laboratory and softbox lights evenly exposed the green screen. Live streaming with chroma-key compositing integrated physical and virtual teaching models into online instruction.

3. Results

3.1. Anatomical analysis

General features: Duplication of the upper portion of the body results in two distinct left and right arms and normal heads (Fig. 3). However, the two upper thoraces merge subcranially resulting in one shared upper midline extremity. The shared hands join at the fifth digit. There is duplication of thoracic structures that merge subdiaphragmatically into a single abdomen, pelvis, and perineum and set of lower extremities.

Osteology: Both twins exhibit a full complement of independent axial skeletal elements (not including ribs, see Table 2) but only a single, shared sternum and lacking observable coccygeal segments (Table 1). Each spine possesses at least a full complement of vertebrae affected by scoliosis (Fig. 4A). Osteological anomalies are widespread in the thoracic region with vertebral bodies showing duplication or absence. Several of the contiguous ribs are fused at the midline or absent (Table 2). Upper limbs are mostly complete and independent except for a shared midline humerus and ulna (Table 2).

Closer inspection of the thoracic regions reveals multiple defects in the bodies and ribs (Table 2; Figs. 4A and 5). The right individual possesses a half T4 vertebral body on the right side resulting in discontinuity in rib attachments so that the fourth rib on the left side articulates with the T5 vertebral body. The left half of the T4 vertebra is absent so the fourth rib articulates with T5. The right individual also possesses T7 with a half-body duplicated on the left side causing discontinuity in rib sequence with the sixth rib articulating with the upper T7 body while the seventh rib articulates with the lower half T7 body. The vertebral column of the right twin includes a total of thirteen vertebrae with twelve ribs on the right side and thirteen ribs on the left side. Rib sequence on the right side shows a full complement of twelve ribs articulating with the corresponding vertebral bodies. However, the rib sequence of the right individual is highly irregular on the left side. In this case, fusion of ribs 6–13 forms a complicated arrangement with the right side of the left individual.

The left twin displays the absence of the right half of the T10 vertebral body as well as its corresponding rib, but a half body at T10 on the left side that articulates with a tenth rib

(Table 2; Figs. 4A and 5). The left twin possesses a duplicated right half body at T12, but this extra osseous structure lacks a corresponding rib. Rib sequence on the left side is normal showing a full complement of twelve ribs. However, the first rib articulates with C7 while ribs 4 and 5 as well as ribs 7–11 are all fused with ribs of the right individual.

Four clavicles and scapulae are present (Fig. 4A, Table 2). The medial arm displays a singular ulna, humerus with a post-mortem break, fused metacarpals, and proximal, intermediate, and distal phalanges in each fifth phalanx while the carpals lack ossification (Table 2). The shared humerus displays double shafts proximally and a fused distal end. Two bilateral innominate bones and corresponding lower extremities are similar in presence and degree of development (Fig. 4A; Table 3).

Cardiopulmonary: Both individuals display a set of bilateral lungs (Fig. 4B). Three lobes are present in the right lung of the right twin while the left lung of the left individual possesses two lobes. The two midline lungs display size reduction without clear demarcation of lobes. Two thymuses are well defined and present bilaterally (Fig. 4B). Two hearts are present with the left individual's heart displaying dextrocardia (Fig. 4B). An ascending aorta arises from each heart, forms an aortic arch and, as they descend, join at the midline subdiaphragmatically at the L1 level of the right individual (Fig. 4C). The venous system displays a single, large umbilical vein entering the abdomen and then courses into the large liver and contributing to a single portal vein (Fig. 4C). A series of hepatic veins are observable and coalesce from right and left sides of the liver to join the portal vein (Fig. 4C).

Digestive System: The twins display a shared digestive system with one large liver that lacks clearly definitive lobulation (Fig. 4D). Foreguts are present but the left individual shows truncation rostral to the diaphragm. The right individual possesses midgut and hindgut structures with a single stomach that displays situs inversus while a single spleen is present on the left. Other peritoneal organs are not clearly visible (Fig. 4D).

Urogenital System: A single urogenital system contains two kidneys with two ureters, one urinary bladder, and one uterus and vagina (Fig. 4E). The kidneys are difficult to discern since they display abnormal rostral-caudal orientations.

Dentition: The dentitions provide a dental age estimation of between eight months in utero and birth based on the amount of incisor and first primary molar calcification, but without any root development for the incisors or calcification of the first permanent molar. (Fig. 4F; Table 4). Thus, the dental eruption pattern corresponds with full term development.

3.2. Case presentation

Rad3D software enables student access to the case presentation for Preparation 296 (Fig. 6). The composite volume model utilizes both transfer function and iso-surface rendering that is observable with a custom WebGL2 Javascript application that downloads and displays models in a compatible browser. Cross sectional radiological planes are selected with observations of either MR or CT images. Previous settings for contrast and rendering tolerance are set by instructors. Embeds, such as streaming videos, 3D models, images,

and links, are optional selections within the report page. Files are accessible using zSpace computers for AR visualization (Fig. 7).

4. Discussion

Preparation 296 is historically relevant, in part, because Dr. Jacob Henle curated the cadaver and students are familiar with the “Loop of Henle” based on their experiences in renal physiology. Background information is provided to the students [23], indicating that Dr. Henle was a charismatic scholar born in Furth, Germany (1809) and matriculated in Medicine at the University of Bonn in 1828. In 1840, he received the appointment of Professor and Director of the newly founded Institute of Anatomy at the University of Zurich in Switzerland. Dr. Henle returned to Germany and accepted a position in the Department of Anatomy at the University of Heidelberg where he significantly contributed to the development of pathology as a scientific discipline and assisted in the establishment of the university’s Pathological Institute. Dr. Henle became a prominent academic figure as he assumed the role of Director of the Anatomy Institute and University of Heidelberg after Institute Director Friedrich Tiedemann. He also performed autopsies for clinicians and was one of the first instructors to integrate histology into the anatomy curriculum [24]. However, Dr. Henle departed from Heidelberg in 1852 regarding the area as too provincial and moved to the University of Gottingen where he discovered and described the renal tubules (ansa nephroni) to which his name was subsequently attributed [23].

Conjoined twinning is a rare occurrence with a frequency ranging from approximately 1:50,000 to 1:100,000 live births [25]. Approximately 35% of all conjoined twin cases result in death within the first 24 h after birth, and 40–60% are stillborn [2]. Classification systems exist, and parapagus conjoined twins have an incidence of 28% of the conjoined twins categories [26]. The underlying mechanism was difficult to comprehend during the mid-19th century when Preparation 296 was curated and examples, such as the craniopagus conjoined twins, did not fit well into concepts of embryology and speciation prior to Darwinian theory [27]. The underlying mechanism remains elusive with various hypotheses proposed [2,28–30]. Renewed interest in this subject occurs due to medical advances, particularly in biomedical imaging, facilitating presurgical planning that increases survival [31,32].

Monozygotic twinning occurs at three critical points [33,34]. First, at the 2-cell or late precompaction stage (4–16 cells), division results in two separate entities including extraembryonic tissues that form separate dichorionic and diamniotic fetuses. This form of twinning occurs in approximately 30% of the monozygotic twinning cases [35]. Second, splitting of the blastocyst results in separate amnions but shared chorions (diamniotic/monochorionic), which is most common and occurs with an incidence of approximately 66%. The least common event occurs later in embryogenesis following the formation of the ectoplacental cone [36] when the fetuses share both the chorion and amnion. In the case of Preparation 296, conjoined twinning could have occurred between 14 and 16 days post-conception due to incomplete separation and duplication of the primitive streak. This observation is based on the presence of double vertebral columns, but a singular large umbilical vein that deviates toward the left individual. The proximally double-shafted and distally fused shared humerus suggest that secondary fusion occurred following the

original conjoined twinning event. Defects in the vertebrae occur more frequently along the medial axis suggesting the occurrence of interactive aplasia [28,37] further supported by the presence of only one spleen on the left side.

The establishment of left-right asymmetry occurs in response to complex expression sequences of several morphogenetic pathways occurring in gastrulation [38]. In mice, nodal cilia establish a leftward cardiac flow [39]. In its absence, cardiac looping reverses, resulting in dextrocardia [40]. The meiosis specific nuclear structural 1 protein (MNS1) is identified as an important factor in establishing left-right asymmetry and may play a key role in situs inversus in humans [41]. In the left individual, dextrocardia affects the left heart while the apex of the right heart displays a typical direction. The incidence of situs inversus is approximately 1 in 8000 [42]. Yet, situs inversus occurs up to 50% in conjoined twins [43]. This high percentage is unlikely if fusion at gastrulation is the underlying event.

The use of VR technology is an efficient method for remote education [14–16]. Conjoined twins provide a useful topic for case-based learning activities consistent with competency-based learning in embryology [44,45]. Manipulation of 3D anatomical models permit complete visualization of structures from various perspectives and depths. VR technology platforms enable visualization of anatomy that are not available through alternate methods [46,47]. This type of technology provides information on specific internal organ structure and development, e.g., observation of the shared digestive system with a foregut that terminated at the diaphragm only in the left individual. VR technology also allows for study and examination at a location and time that is convenient to the student while 3D printing is also possible for further understanding of complex spatial relationships [12]. Limitations may include prohibitive cost and restricted access to electronic equipment and devices. However, the system described here is viewable using a browser and phone readily available to most students. Another limiting factor could be differential shrinkage of the museum specimen occurring because of the fixative used in collection.

Utilization of an online and remote approach is highly convenient for study and analysis of anatomical structures [48]. A variety of virtual platforms allow for collaboration and visualization of structures. Rad3D is a DICOM viewer accessible from mobile devices. Sketchfab is also a virtual platform that is emerging as a hub for sharing 3D anatomical models. Online platforms allow for more accessibility to information by a wider audience range while Creative Commons access for academic applications. The use of augmented reality technology based on medical museum collections is becoming a reality [49]. This provides a unique opportunity for collaborative research and ethical post-mortem examination. In-person instructional limitations, such as those imposed by the COVID-19 pandemic, can be overcome through online student collaborations ensuring safe educational experiences.

In conclusion, the described workflow provides an effective approach for generating ease-of-use XR models of historically relevant museum specimens. Digital distribution of visualizations occurs using device agnostic software achieving widespread availability. Sufficient anatomical detail is present, enabling online case presentation within the medical curriculum. Anecdotal student comments indicate that case presentation is engaging and

thought provoking, although instructional effectiveness is not assessed. Future work will focus on the development of a case-based library of old and rare museum specimens that students can access to explore topics involving developmental, anatomical, and public health concepts.

Acknowledgements

Beth K. Lozanoff, CMI, assisted with figure production and presentation. Drs. Vernadeth Alarcon, Yusuke Marikawa and Dave Bolender provided helpful comments on earlier versions of the manuscript and regarding embryology of conjoined twins. Ms. Tina Henle (tinahenle.com) graciously provided the previously unpublished family portrait of Dr. Jacob Henle. Prof. Fritz Dross, Erlangen-Nürnberg, and Prof. Iris Ritzmann, Zürich, graciously provided assistance concerning references related to Dr. Henle's academic contributions.

Funding

This work was supported in part by grants from the National Institutes of Health (NIH) and the National Institute of General Medical Sciences (NIGMS) [award number: P20GM 103466].

References

- [1]. Marreez YMAH, Willems LNA, Wells MR, The role of medical museums in contemporary medical education, *Anat. Sci. Educ* 3 (2010) 249–253, 10.1002/ase.168. [PubMed: 20814912]
- [2]. Boer LL, de Rooy L, Oostra RJ, Dutch teratological collections and their artistic portrayals, *Am. J. Med. Genet. C. Semin. Med. Genet* 187 (2021) 283–295, 10.1002/ajmg.c.31902. [PubMed: 33982861]
- [3]. Boer LL, Schepens-Franke AN, Oostra RJ, Two is a crowd: on the enigmatic etiopathogenesis of conjoined twinning, *Clin. Anat* 32 (2019) 722–741, 10.1002/ca.23387. [PubMed: 31001856]
- [4]. Pooh RK, Shiota K, Kurjak A, Imaging of the human embryo with magnetic resonance imaging microscopy and high-resolution transvaginal 3-dimensional sonography: human embryology in the 21st century, *Am. J. Obstet. Gynecol* 204 (2011), 10.1016/j.ajog.2010.07.028, 77.E1–77.E16. [PubMed: 20974463]
- [5]. Gasser RF, Cork RJ, Stillwell BJ, McWilliams DT, Rebirth of human embryology, *Anat. Rec.* 243 (2014) 621–628, 10.1002/dvdy.24110.
- [6]. de Bakker BS, de Jong KH, Hagoort J, de Bree K, Besselink CT, de Kanter FEC, Veldhuis T, Bais B, Schildmeijer R, Ruijter JM, Oostra RJ, Christoffels VM, Moorman AFM, An interactive three-dimensional digital atlas and quantitative database of human development, *Science* 354 (2016), 10.1126/science.aag0053.
- [7]. Chhem RK, Woo JKH, Pakkiri P, Stewart E, Romagnoli C, Garcia B, CT imaging of wet specimens form a pathology museum: how to build a “virtual museum” for radiopathological correlation teaching, *HOMO- J. Comp. Hum. Biol.* 57 (2006) 201–208, 10.1016/j.jchb.2006.03.003.
- [8]. Jutras LC, Magnetic resonance of hearts in a jar: breathing new life into old pathological specimens, *Cardiol. Young* 20 (2010) 275–283, 10.1017/S1047951109991521. [PubMed: 20346199]
- [9]. Tomaka A, Luchowski L, Skabek K, From Museum exhibits to 3D models, in: Cyran KA, Kozielski S, Peters JF, Stanczyk U, Wakulicz-Deja A (Eds.), *Man-Machine Interactions, Adv. Intell. Syst.*, vol. 59, Springer, Berlin, Heidelberg, 2009, pp. 477–486, 10.1007/978-3-642-00563-3_50.
- [10]. Jocks I, Livingstone D, Rea PM, An Investigation to Examine the Most Appropriate Methodology to Capture Historical and Modern Preserved Anatomical Specimens for Use in the Digital Age to Improve Access: a Pilot Study, *Proceedings of the INTED2015 Conference, Madrid, Spain, 2015*, ISBN 978-84-606-57637, pp. 6377–6386.
- [11]. Pearlstein KE, Simmons-Ehrhardt T, Spatola BF, Means BK, Mani MR, Modernizing medical museums through the 3D digitization of pathological specimens, in: Rea PM

- (Ed.), *Biomedical Visualisation*, Adv. Exp. Med. Biol, vol. 1334, Springer, Cham, 2021, 10.1007/978-3-030-76951-2_9.
- [12]. Elsayed M, Kadom N, Ghobadi C, Strauss B, Dandan OA, Aggarwal A, Anzai Y, Griffith B, Lazarow F, Straus CM, Safdar NM, Virtual and augmented reality: potential applications in radiology, *Acta Radiol.* 61 (2020) 1258–1265, 10.1177/0284185119897362. [PubMed: 31928346]
- [13]. Wish-Baratz S, Gubatina AP, Enterline R, Griswold MA, A new supplement to gross anatomy dissection: *HoloAnatomy*, Med, Educ. Next 53 (2019) 522–523, 10.1111/medu.13845.
- [14]. Caudell TP, Summers KL, Holten IV J, Hakamata T, Mowafi M, Jacobs J, Lozanoff BK, Lozanoff S, Wilks D, Keep MF, Saiki S, Alverson D, Virtual patient simulator for distributed collaborative medical education, *Anat. Rec.* 270 (2003) 23–29, 10.1002/ar.b.10007.
- [15]. Alverson DC, Saiki SM Jr., Kalishman S, Lindberg M, Mennin S, Mines J, Serna L, Summers K, Jacobs J, Lozanoff S, Lozanoff B, Saland L, Mitchell S, Umland B, Greene G, Buchanan HS, Keep M, Wilks D, Wax DS, Coulter R, Goldsmith TE, Caudell TP, Medical students learn over distance using virtual reality simulation, *Simulat. Healthc. J. Soc. Med. Simulat.* 3 (2008) 10–15, 10.1097/SIH.0b013e31815f0d51.
- [16]. Nakamatsu N, Aytac G, Mikami B, Thompson JD, Davis III M, Rettenmeier C, Maziero D, Stenger VA, Labrash S, Lenze S, Torigoe T, Lozanoff BK, Kaya B, Smith A, Miles JD, Lee UY, Lozanoff S, Case-based radiological anatomy instruction using cadaveric MRI imaging and delivered with extended reality web technology, *Eur. J. Radiol.* 146 (2022) 110043, 10.1016/j.ejrad.2021.110043. [PubMed: 34844172]
- [17]. Kölliker A, *Handbuch der Gewebelehre des Menschen*, vol. 4, Umgearb. Aufl. Leipzig, 1863, pp. 520–521.
- [18]. Dreger AD, *One of Us Conjoined Twins and the Future of Normal*, Harvard University Press, Cambridge, Massachusetts, 2004, ISBN 0-674-01825-7.
- [19]. Schour I, Massler M, The development of the human dentition, *J. Am. Dent. Assoc* 28 (1941) 1153–1160.
- [20]. Eli I, Sarnat H, Talmi E, Effect of the birth process on the neonatal line in primary tooth enamel, *Pediatr. Dent* 11 (1989) 220–223. [PubMed: 2638008]
- [21]. Proffit WR, Fields HW, Sarver DM, *Contemporary Orthodontics*, fourth ed., Mosby Elsevier, St. Louis, Montgomery, 2007.
- [22]. AlQahtani SJ, Hector MP, Liversidge HM, Brief Communication: the London Atlas of human tooth development and eruption, *Am. J. Phys. Anthropol.* 142 (2010) 481–490, 10.1002/ajpa.21258. [PubMed: 20310064]
- [23]. Robinson V, *The Life of Jacob Henle*, NY: Medical Life Company, New York, 1921.
- [24]. Doll S, Ein eher kurzes gastspiel: Jacob Henle in Heidelberg, in: Doll S, Kirsch J, Eckart WU (Eds.), *Wenn der Tod dem Leben dient-Der Mensch als Lehrmittel*, Springer, Berlin, 2017, ISBN 978-3-8253-6135-8, pp. 37–39.
- [25]. Mathew RP, Francis S, Basti RS, Suresh HB, Rajarathnam A, Cunha PD, Rao SV, Conjoined twins - role of imaging and recent advances, *J. Ultrason.* 17 (2017) 259–266, 10.15557/JoU.2017.0038. [PubMed: 29375901]
- [26]. Karaer A, Tanrikulu I, Gunes N, Cakir E, Oztas A, Parapagus dicephalus dibrachus dipus: a case of conjoined twins, *J. Turk. Ger. Gynecol. Assoc.* 10 (2009) 241–243. [PubMed: 24591881]
- [27]. Richards E, A political anatomy of monsters, hopeful and otherwise: teratology, transcendentalism, and evolutionary theorizing, *Isis* 85 (1994) 377–411. [PubMed: 7960661]
- [28]. Machin GA, Sperber GH, Lessons from conjoined twins, *Am. J. Med. Genet.* 28 (1987) 89–97, 10.1002/ajmg.1320280113. [PubMed: 3674121]
- [29]. Spencer R, Theoretical and analytical embryology of conjoined twins: Part I: Embryogenesis, *Clin. Anat* 13 (2000) 36–53, 10.1002/ajmg.1320280113. [PubMed: 10617886]
- [30]. Kaufman MH, The embryology of conjoined twins, *Childs Nerv. Syst.* 20 (2004) 508–525, 10.1007/s00381-004-0985-4. [PubMed: 15278382]
- [31]. McHugh K, Kiely EM, Spitz L, Imaging of conjoined twins, *Pediatr. Radiol* 36 (2006) 899–910, 10.1007/s00247-006-0121-6. [PubMed: 16622666]

- [32]. Rabeeah AA, Conjoined twins - past, present and future, *J. Pediatr. Surg.* 41 (2006) 1000–1004, 10.1016/j.jpedsurg.2005.12.045. [PubMed: 16677900]
- [33]. Machin GA, Some causes of genotypic and phenotypic discordance in monozygotic twin pairs, *Am. J. Med. Genet.* 61 (1996) 216–228, 10.1002/(SICI)1096-8628(19960122)61:3<216::AID-AJMG5>>3.0.CO;2-S. [PubMed: 8741866]
- [34]. Scott L, The origin of monozygotic twinning, *Reprod. Biomed. Online* 5 (2002) 276–284, 10.1016/S1472-6483(10)61833-0.
- [35]. Luebke HJ, Reiser CA, Pauli RM, Fetal Disruptions: assessment of frequency, heterogeneity, and embryologic mechanisms in a population referred to a community-based stillbirth assessment program, *Am. J. Med. Genet.* 36 (1990) 56–72, 10.1002/ajmg.1320360113. [PubMed: 2333908]
- [36]. Cross JC, How to make a placenta: mechanisms of trophoblast cell differentiation in mice—A review, *Placenta* 26 (2005), 10.1016/j.placenta.2005.01.015. S3–S9. [PubMed: 15837063]
- [37]. Oostra RJ, Keulen N, Jansen T, van Rijn RR, Absence of the spleen(s) in conjoined twins: a diagnostic clue of laterality defects? Radiological study of historical specimens, *Pediatr. Radiol* 42 (2012) 653–659, 10.1007/s00247-011-2316-8. [PubMed: 22237480]
- [38]. Brand T, Heart development: molecular insights into cardiac specification and early morphogenesis, *Dev. Biol.* 258 (2003) 1–19, 10.1016/S0012-1606(03)00112-X. [PubMed: 12781678]
- [39]. Supp DM, Witte DP, Potter SS, Brueckner M, Mutation of an axonemal dynein affects left-right asymmetry in inversus viscerum mice, *Nature* 389 (1997) 963–966, 10.1038/40140. [PubMed: 9353118]
- [40]. Nonaka A, Shiratori H, Saijoh Y, Hamada H, Determination of left-right patterning of the mouse embryo by artificial nodal flow, *Nature* 418 (2002) 96–99, 10.1038/nature00849. [PubMed: 12097914]
- [41]. Leslie JS, Rawlins LE, Chioza BA, Olubodun OR, Salter CG, Fasham J, Jones HF, Cross HE, Lam S, Harlalka GV, Muggenthaler MMA, Crosby AH, Baple EL, MNS1 variant associated with situs inversus and male infertility, *Eur. J. Hum. Genet.* 28 (2020) 250–255, 10.1038/s41431-019-0489-z.
- [42]. Perloff JK, The cardiac malformations, *Am. J. Cardiol.* 108 (2011) 1352–1361, 10.1016/j.amjcard.2011.06.055. [PubMed: 21861958]
- [43]. Seo JW, Shin SS, Chi JG, Cardiovascular system in conjoined twins: an analysis of 14 Korean cases, *Teratology* 32 (1985) 151–161, 10.1002/tera.1420320202. [PubMed: 3840285]
- [44]. Das M, Claeson KM, Lowrie DJ Jr., Bolender DL, Fredieu JR, Guttman G, Conway ML, Ghosh T, Edmondson AC, Cork RJ, Rengasamy P, Lee LMJ, Williams JM, Oberg KC, A guide to competencies, educational goals, and learning objectives for teaching human embryology in an undergraduate medical education setting, *Med. Sci. Educ.* 28 (2018) 417–428, 10.1007/s40670-018-0542-5.
- [45]. Holland JC, Smith C, O’Shea M, Stewart J, Ockleford C, Finn GM, The anatomical society core embryology syllabus for undergraduate medicine, *J. Anat.* 235 (2019) 847–860, 10.1111/joa.13023. [PubMed: 31218692]
- [46]. Lozanoff S, Lozanoff BK, Sora MC, Rosenheimer J, Keep MF, Tregear J, Saland L, Jacobs J, Saiki S, Alverson D, Anatomy and the Access Grid: exploiting plastinated brain sections for use in distributed medical education, *Anat. Rec.* 270B (2003) 30–37, 10.1002/ar.b.10006.
- [47]. Hong T, Bezaud G, Lozanoff BK, Labrash S, Lozanoff S, Presentation of anatomical variations using the aurasma mobile app, *Hawai’i J. Med. Public Health* 74 (2015) 16–21.
- [48]. Trelease RB, From chalkboard, slides, and paper to e-learning: how computing technologies have transformed anatomical sciences education, *Anat. Sci. Educ.* 9 (2016) 583–602, 10.1002/ase.1620. [PubMed: 27163170]
- [49]. Sugiura A, Kitama T, Toyoura M, Mao X, The use of augmented reality technology in medical museums, in: Chan LK, Pawlina W (Eds.), *Teaching Anatomy A Practical Guide*, Springer, Cham, 2020, pp. 337–347, 10.1007/978-3-030-43283-6.



B 296. Mit der Brust verwachsene Zwillinge mit verschmolzenen hinteren Armen und einfachen unteren Ende.

Fig. 1.
 A) Portrait of Dr. Henle circa 1844 (courtesy of Ms. Tina Henle). B) Description of the conjoined twins' cadaver in his Journal for Pathological Preparations under entry Preparation 296: "Mit der Brust verwachsene Zwillinge mit verschmolzenen hinteren Armen und einfachen unteren Ende" (Twins with merged breasts and fused back arms and simple lower end).

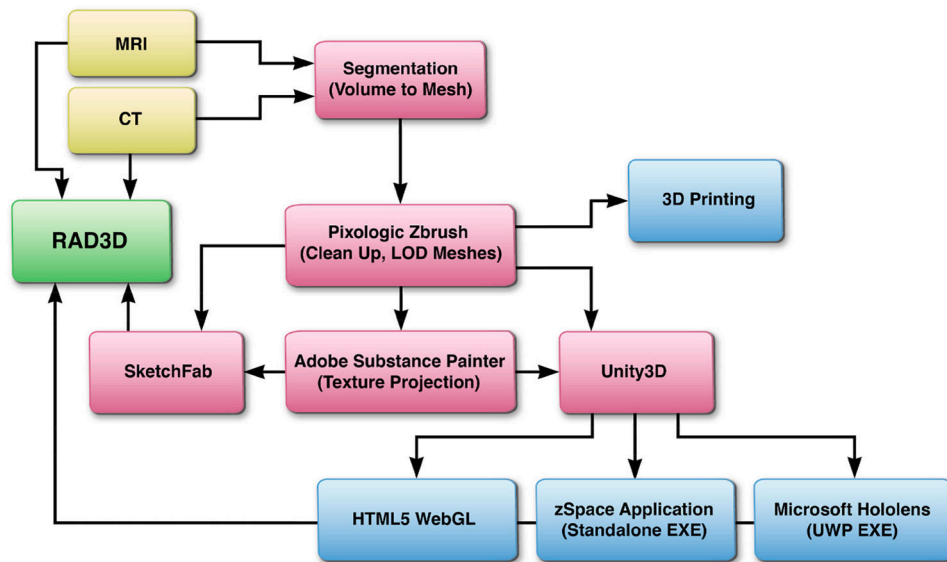


Fig. 2. Workflow for image capture (yellow), segmentation and modeling (red), and XR visualization (blue). The online case is compiled and distributed using Rad3D software (green).

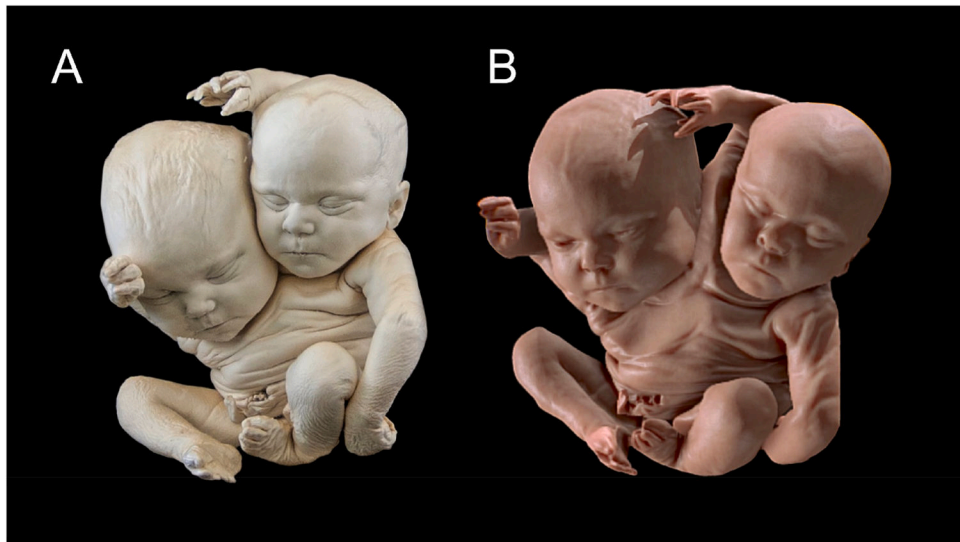


Fig. 3. The parapagus dicephalus tribrachius dipus conjoined twins' cadaver visualized with a photograph (A) and computer model (B) showing a high degree of surface consistency between images.

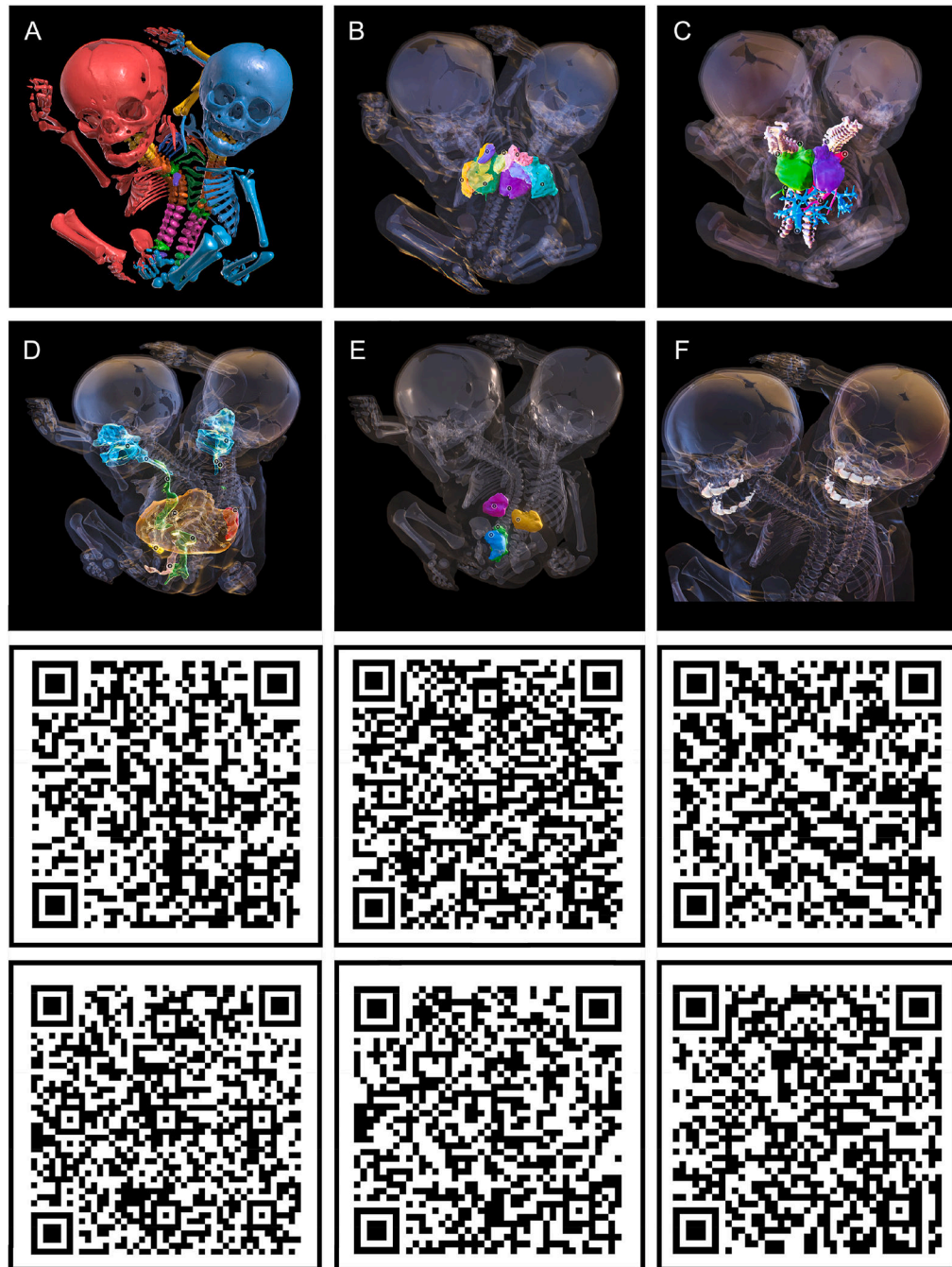


Fig. 4. XR models of the developing systems used in the case study including osteology (A), cardiopulmonary (B, C), gastrointestinal (D), urogenital (E) and dental (F). Interactive models are accessible using the QR codes or links.

A) <https://sketchfab.com/3d-models/osteology-of-parapagus-conjoined-twins-84b414f05ac54d9f8173fca017d7c7f8>

B) <https://sketchfab.com/3d-models/pulmonary-system-dicephalic-parapagus-twins-1f3f36b287084e31ad97e444ab467e0b>

- C) <https://sketchfab.com/3d-models/cardiovascular-system-of-parapagus-twins-3645181d719d4b4f94d4285fd02924f7>
- D) <https://sketchfab.com/3d-models/gi-system-or-dicephalic-parapagus-conjoined-twin-72932b457cd749e79dffa54285e43d2>
- E) <https://sketchfab.com/3d-models/ug-system-for-dicephalic-parapagus-twins-42cb6313a3fc460f9aea02f85d679cfc>
- F) <https://sketchfab.com/3d-models/conjoined-twins-teeth-59cd79a5781646789eeacd6b624e9fdf>.

Right individual			
rt. Rib	vertebral body		lt. rib
	rt. half	lt. half	
1	T1	T1	1
2	T2	T2	2
3	T3	T3	3
4	T4 (extra half body)		
5	T5	T5	4
6	T6	T6	5
7	T7	T7 (duplicated half body)	6f
8	T8	T8	7f
9	T9	T9	8f
10	T10	T10	9f
11	T11	T11	10f
12	T12	T12	11f
	T13	T13	12f
Total			
12	13	13	13

Left individual			
rt. Rib	vertebral body		lt. rib
	rt. half	lt. half	
1	C7	C7	
2	T1	T1	1
3	T2	T2	2
4f	T3	T3	3
5f	T4	T4	4
6	T5	T5	5
7f	T6	T6	6
8f	T7	T7	7
9f	T8	T8	8
10f	T9	T9	9
		T10 (extra half body)	10
11f	T11	T11	11
12	T12	T12 (duplicated half body)	12
Total			
12	13 (1 C and 12 T)	12	12

f. the rib fused with the other individual's rib

Fig. 5. Schematic comparison of vertebrae and rib anomalies in the conjoined twins.

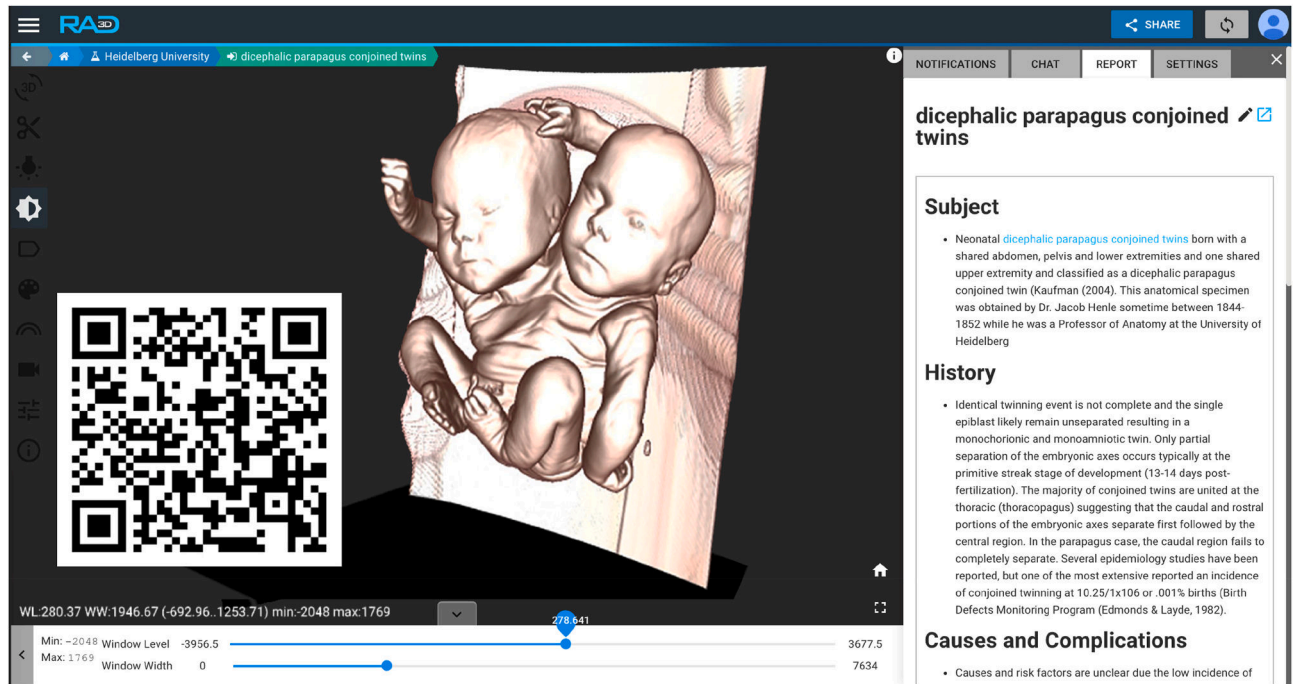


Fig. 6. Rad3D user interface for the embryological case presentation. DICOM slices are rendered as a volumetric in the workspace while the user simultaneously views the cross sections. The report is presented in the right frame and provides radiological, pathological, and anatomical information as well as external links. Rad3D interface is accessible using the QR code or link.

<https://rad3d.com/a/view/E870EB90-19A8-46E2-B035-906A409986CE>.



Fig. 7. The DICOM viewing software is viewed on a zSpace computer to provide XR visualizations. The video demonstration is accessible using the QR code or link. <https://youtu.be/GYOUw2fOhrc>.

Table 1

Developmental assessment of axial skeletal elements (not including ribs, see Table 2). Right (R), Left (L), Present (+), Absent (-).

Region	Bone	R Twin	Fused	L Twin
Skull	Cranium	+	-	+
	Mandible	+	-	+
Hyoid	Hyoid bone	+	-	+
Cervical	C1	+	-	+
	C2	+	-	+
	C3	+	-	+
	C4	+	-	+
	C5	+	-	+
	C6	+	-	+
	C7	+	-	+
Thoracic	T1	+	-	+
	T2	+	-	+
	T3	+	-	+
	T4	+	-	+
	T5	+	-	+
	T6	+	-	+
	T7	+	-	+
	T8	+	-	+
	T9	+	-	+
	T10	+	-	+
	T11	+	-	+
	T12	+	-	+
Lumbar	L1	+	-	+
	L2	+	-	+
	L3	+	-	+
	L4	+	-	+
	L5	+	-	+
Sacrum-Coccyx	S1	+	-	+
	S2	+	-	+
	S3	+	-	+
	S4	+	-	+
	S5	+	-	-
	Coccyx	-	-	-
Sternum	Sternum	-	+	-

Table 2

Developmental assessment of the Ribs and Upper Extremity. Right (R), Left (L), Present (+), absent (-).

Region	Bone	R Twin		Fused	L Twin	
		R	L		R	L
Rib	1st	+	+		+	+
	2nd	+	+		+	+
	3rd	+	+		+	+
	4th	+	+	R6-L4		+
	5th	+	+	R7-L5		+
	6th	+			+	+
	7th	+		R8-L7		+
	8th	+		R9-10-L8		+
	9th	+		R11-L9		+
	10th	+		R12-L10		+
	11th	+		R13-L11		+
	12th	+			+	+
Shoulder girdle	Clavicle	+	+	-	+	+
	Scapula	+	+	-	+	+
Arm	Humerus	+		R-L		+
	Radius	+	+	-	+	+
	Ulna	+		R-L		+
Carpals	Scaphoid	-	-	-	-	-
	Lunate	-	-	-	-	-
	Triquetral	-	-	-	-	-
	Pisiform	-	-	-	-	-
	Trapezium	-	-	-	-	-
	Trapezoid	-	-	-	-	-
	Capitate	-	-	-	-	-
	Hamate	-	-	-	-	-
Metacarpals	I	+		R-L	+	+
	II	+	+	-	+	+
	III	+	+	-	+	+
	IV	+	+	-	+	+
	V	+	+	-	+	+
Proximal phalanges	I	+	+	-	+	+
	II	+	+	-	+	+
	III	+	+	-	+	+
	IV	+	+	-	+	+
	V	+	+	-	+	+
Middle phalanges	II	+	+	-	+	+
	III	+	+	-	+	+
	IV	+	+	-	+	+

Region	Bone	R Twin		Fused	L Twin	
		R	L		R	L
	V	+	+	-	+	+
Distal phalanges	I	+	+	-	+	+
	II	+	+	-	+	+
	III	+	+	-	+	+
	IV	+	+	-	+	+

Author Manuscript

Author Manuscript

Author Manuscript

Author Manuscript

Table 3

Developmental assessment of the Hip and Lower Extremity. Right (R), Left (L), Present (+), absent (-), undetermined (?).

Region	Bone	R Twin		L Twin	
		R	L	R	L
Hip	Ilium	+		+	
	Pubis	+		+	
	Ischium	+		+	
Thigh & Leg	Femur	+		+	
	Patella	-		-	
	Tibia	+		+	
	Fibula	+		+	
Tarsals	Cuboid	-		-	
	Talus	+		+	
	Calcaneus	+		+	
	Navicular	-		-	
	Medial cuneiform	-		-	
	Intermediate cuneiform	-		-	
	Lateral cuneiform	-		-	
Metatarsals	I	+		+	
	II	+		+	
	III	+		+	
	IV	+		+	
	V	+		+	
Foot proximal phalanges	I	+		+	
	II	+		+	
	III	+		+	
	IV	+		+	
	V	+		+	
Foot middle phalanges	II	+		+	
	III	+		+	
	IV	+		+	
	V	?		?	
	Foot distal phalanges	I	+		+
II		+		+	
III		+		+	
IV		+		+	
V		?		?	

Table 4

Fraction (%) of the dental crown calcification for age estimation. Right (R); Left (L).

Tooth	% of Crown Calcification	
	R Twin	L Twin
A	1/8	1/8
B	1/2	1/2
C	1/3	1/3
D	1/2	1/2
E	3/4	3/4
F	3/4	3/4
G	1/2	1/2
H	1/3	1/3
I	1/2	1/2
J	1/8	1/8
K	1/8	1/8
L	1/4	1/4
M	1/3	1/3
N	1/2	1/2
O	1/2	1/2
P	1/2	1/2
Q	1/2	1/2
R	1/3	1/3
S	1/4	1/4
T	1/8	1/8
Age Estimate	8 months in utero to birth	

Author Manuscript

Author Manuscript

Author Manuscript

Author Manuscript